Civil and Environmental Research
ISSN 2224-5790 (Paper) ISSN 2225-0514 (Online)
Vol.3, No.7, 2013

Kinetic Modelling of Nitrate Removal from Aqueous Solution during Electrocoagulation

Ghanim, A.N. and Ajjam, S.K.*
Electrochemical Eng. Dep., Eng. College, Babylon University, Hilla 51002, PO box 4, Iraq
* E-mail of the corresponding author: satajam58@yahoo.com

Abstract

The present study focuses on the prediction of mathematical model that describes the nitrate removal from an aqueous solution by means of electrochemical techniques. The nitrate removal was modeled by applying the kinetic reaction rate equations and the adsorption isotherms. The experimental part of this study was implied to investigate the performance of nitrate removal from an aqueous solution by utilizing an electrochemical method (i.e. electrocoagulation). Experiments were carried out to treat a synthetic strength aqueous solution of 150 mg/l NO_3^- concentration through batchwise mode. The nitrates removal from aqueous solution was studied as a function of the electrocoagulation time, and the applied current density with iron MP-P connected electrodes. The theoretical part of this study was attempted to conform the nitrate removal data to Langergren pseudo first order, Ho pseudo second order and Elovich kinetic models. The equilibrium results were analyzed by the adsorption isotherms Langmuir, Freundlich and Temkin. Based on correlation coefficient, it has been found that the NO_3^- electrocoagulation with ferric(III) hydroxides adsorbent can be extremely represented by the pseudo second order reaction kinetic model, and the equilibrium data found better fit to Freundlich equilibrium isotherm.

Key words: NO_3^- removal, Electrocoagulation, kinetic models, adsorption isotherms.

1. Introduction

In many sources of water, nitrate contamination is a widespread environmental problem especially in areas of intensive agriculture. Nitrate can cause serious health problems in humans such as the “blue baby syndrome” in infants, liver damage and cancer (Miao Lia et al., 2010). Nitrate is a stable and highly soluble ion with low potential for co-precipitation or adsorption. These properties make it difficult to be removed from water. Therefore, treatment for nitrate is typically very complicated and expensive (El-Shazly et al., 2011). Existing methods of removing nitrate from wastewater include an ion exchange, biological decomposition, reverse osmosis, electrodialysis and catalytic denitrification. Although the ion exchange resin is efficient process preferred for treatment of groundwater, it is costly with undesirable high residual constituents in the treated water (Liang et al., 1999). The biological decomposition method is extremely effective process for treatment of surface waters. Unfortunately, this process is generally time consuming. It limited in temperature ranges; requires extensive maintenance (Canter, 1997, Miao Lia et al., 2010). Reverse osmosis and Electrodialysis can be used to an efficiency of about 65% nitrate removal, however an extremely high cost is needed for energy input (Horold et al., 1993).

Electrocoagulation process has been successfully employed for colored, heavy metals and COD removal of industrial wastewaters (Lin and Wu, 1996). The Electrocoagulation technique has several advantages including the ability to deliver a precise coagulant dose via control of the amount of applied electrical current, easy automation, low energy requirements, and the ability to destabilize, aggregate, and separate the pollutants in a single stage (Mollah et al., 2004, Canizares et al., 2006, Can et al., 2006).

Electrocoagulation was investigated for its performance in the removal of NO_3^- from wastewater using vertical cylindrical monopolar Aluminium electrodes in a batch electrocoagulation unit (El-Shazly et al., 2011). They showed that the removal efficiency percentage of the NO_3^- has been increased by increasing the initial solution pH and the current density. The paper mill effluents contain pollutants like phosphate, ammonium, nitrate, BOD and COD (Mehmet Uğurlu, 2004). The removal was investigated by different current intensity, electrodes (Al and Fe) and electrolysis time. It was generally observed that an increase in removal efficiency is associated with an increase in current intensity. Full removal of nitrate was possible but with higher energy consumption for electroreduction and electrocoagulation methods (Koparal and Ogutveren, 2002). They showed that the removal of NO_3^- from water to an allowable concentration has been accomplished at the pH range of 5-7 by electroreduction method while in the electrocoagulation method, an allowable concentration of NO_3^- has been achieved at the pH range of 9-11. Also, they showed that the reduction of NO_3^- to N_2 gas can be possible and the NO_3^- removal has been accomplished with precipitation of $Fe(OH)_3$ produced in water by soluble anode. The optimum conditions for NO_3^- removal efficiency were tested on Kerman water with Al electrodes (Malakootian et al., 2011). They showed that the EC process can reach NO_3^- to less than standard limit and the NO_3^- removal efficiency increases with increase of the electrical potential difference. In contrast, the NO_3^- removal efficiency decreases with an increase of NO_3^- initial concentration. Despite increased - NO_3^- initial concentration, the requirement time for achieving the desired amount of remaining NO_3^- increases. The same result was obtained but with simultaneous removal of Cr^{6+} and NO_3^- from an aqueous solution by EC using Al as anode (Abbas Rezaee et al., 2011). The removal of both Cr^{6+} and NO_3^- increased with an increase in the current intensity, time and maximum removal efficiency of NO_3^- achieved at high pH values. For both ions, the efficiency was over 90%. In most electrochemical processes, current intensity and electrolysis time are the most important parameters for controlling the reaction rate (Emamjomeh, M. and Sivakumar, M., 2009). They designed a laboratory batch electrocoagulation/flotation (ECF) reactor to investigate the effects of different parameters such as electrolysis time, electrolyte pH, initial NO_3^- concentration, and current rate on the NO_3^- removal efficiency. The results showed that the NO_3^- removal by ECF process followed a simple first order process and the main mechanism of NO_3^- removal was Al oxidation at the anode that can decompose and reduce NO_3^- from water.

Electrochemical treatment is an effective method for the removal of NO_3^- from aqueous solutions (Miao Lia et al., 2010). Reduction of NO_3^- and anodic oxidation of the formed by-product in an undivided cell was studied in the presence of NaCl. The Box–Behnken design was employed to develop mathematical models for predicting electrochemical NO_3^- removal geometry. In contrast, a divided cell was studied for NO_3^- removal from groundwater using electrolytic reduction method (Prasad, 2005). The process involves the generation of H_2 gas at the copper cathode that reduces the NO_3^- to N_2 while the anode was insoluble triple mixed oxide.

The aim of this study was to determine the performance of electrocoagulation process in nitrate removal and to predict a well fit mathematical models that describe the kinetic and mechanism of nitrate removal from aqueous solution by means of EC techniques with various operating conditions.

2. Experimental set up

The used electrocoagulator cell (figure-1) was 1250 ml glass reactor with upper Teflon cover containing four glands for electrodes fixation (the separation between the anode and the cathode was kept constant at 2cm, equipped with magnetic stirrer (HP-3000) without temperature control. The electrolysis time was established of 70 minutes using DC Regulated Power Supply (QJE-QI5030S 0-50V/30A) and a current controlled through rheostat (Wheatstone Type 2755-Japan). The current was kept invariant in each test by a rheostat and measured by Digital Multimeter (VICTOR-70C). Four electrodes of iron having the dimensions of 30×150×1 mm operated with monopolar parallel (MP-P) connection mode.

3. Material and Procedure

In all stages of the study, the electrical potential difference was applied and measured by voltmeter and the current densities were fixed to 2, 4, 6, 8 and 10 mA/cm^2 through rheostat connected with ohmmeter and installed on circuit. However, in each run, one litre of aqueous nitrate solution was used to treat by electrocoagulation process. The solution in the reactor was stirred by a magnetic plate stirrer with Teflon bar at a rotating velocity of 100 rpm. Controlled direct current was supplied by a DC power supply. The cell arrangement can study the effect of the EC process on nitrate removal efficiencies using two variables: current density (mA/cm^2) and EC operation time (minutes). The electrical potential was held constant for each run, being fixed at 15 volts. The synthetic aqueous solution was prepared by sodium nitrate and deionized water in 150 mg/l concentration.

In all stages of the study, sodium chloride was added to solution in 200 mg/l concentration as a support electrolyte due to low electrical conductivity. The pH was adjusted to a value of 8 with 1M NaOH. Before each run the electrodes were treated with 15%-wt HCl for cleaning and they are washed with distilled water prior to use. All EC batch experimental runs were performed at ambient temperature (290 K) in the laboratory. Initially the synthetic aqueous solution was rigorously stirred for 5 minutes by stirrer for homogenization of sample.

4. Analysis and Calculation

All experiments were carried out under potentiostatic conditions covering a range of electocoagulation operating time of 10, 20, 30, 40, 50, 60 and 70 minutes. Nitrates were determined by standard colorimetric method a U.V. Spectrophotometer (UV-1800 SHIMADZU, JAPAN), 5 ml samples were drawn at different time intervals, diluted to 50 ml with distilled water, filtered to remove any possible interference from suspended particles, then acidified with 1ml 1N HCl to prevent interference from hydroxides. A calibration curve was prepared for the NO_3^- concentration range used by adjusting the wave length at 220 nm. That curve was used for finding out the NO_3^- concentration at any time. The calculation of nitrate removal efficiencies after electrocoagulation treatment was performed using the following formula:

$$\%NR = (\frac{C_o - C}{C_o}) \times 100 \qquad (1)$$

Where %NR is NO_3^- removal percent, C_o and C are concentrations of NO_3^- before and after electrocoagulation.

5. Electrocoagulation Mechanism

The pollutant is generally adsorbed at the surface of the flocs (coagulant) generated electrochemically.

Critical analysis of the electrocoagulation of a pollutant reveals that there are two separate processes taking place (Chithra and Balasubramanian, 2010), i.e. electrochemical process through which the metal coagulants are generated and physio-chemical process through which the effluents are adsorbed on the surface of the coagulants. The following equations are an illustration of this phenomenon (Canton, 2010):

(a) Mechanism (1):

Anode: $Fe_{(s)} \rightarrow Fe^{+2}_{(aq)} + 2e^-$

$Fe^{+2}_{(aq)} + 2OH^-_{(aq)} \rightarrow Fe(OH)_{2(s)}$

Cathode: $2H_2O_{(l)} + 2e^- \rightarrow H_{2(g)} + 2OH^-_{(aq)}$

Overall: $Fe_{(s)} + 2H_2O_{(l)} \rightarrow Fe(OH)_{2(s)} + H_{2(g)}$

Fe is released to solution as Fe(II) and is then oxidized to Fe(III) by the dissolved O_2 (Wei Wan,2010) and by hypochlorous acid formed due to chloride oxidation (Evrim Yüksel et al., 2009) :

Oxidation: $2Cl^- \rightarrow Cl_2 + 2e^-$

$Cl_{2(g)} + H_2O \rightarrow HOCl + H^+ + Cl^-$

$Fe(OH)_2 + HOCl \rightarrow Fe(OH)_{3(s)} + Cl^-$

(b)Mechanism (2):

Anode: $4Fe_{(s)} \rightarrow 4Fe^{+2}_{(aq)} + 8e^-$

$4Fe^{+2}_{(aq)} + 10H_2O_{(l)} + O_{2(g)} \rightarrow 4Fe(OH)_{3(s)} + 8H^+_{(aq)}$

Cathode: $8H^+_{(aq)} + 8e^- \rightarrow 4H_{2(g)}$

Overall: $4Fe_{(s)} + 10H_2O_{(l)} + O_{2(g)} \rightarrow 4Fe(OH)_{3(s)} + 4H_{2(g)}$

The Fe^{2+} cation hydrolyses in water to form hydroxo-amorphous polymeric complexes (flocs) with the adsorbed nitrates and can be precipitated from water, such as:

$$nFe(OH)_{3(S)} + NO^-_{3(aq)} \rightarrow [Fe_n(OH)_{3n}.NO_3^-]_{(S)}$$

Once the flocs are generated, the H_2 gas binds and creates a buoyant force on the flocs leading to its flotation and ultimately to the removal of the NO_3^- as a floc-foam layer at the liquid surface.

$$Floc + H_{2(g)} \rightarrow Floats$$

Other flocs that are heavier settle at the bottom of the cell (Canton K. W., 2010).

The electrode consumption can be estimated according to Faraday’s law and the amount of coagulant generated can be estimated stoichiometrically (Parga et al., 2009):

$$W = \frac{(I \times t \times M)}{z \times F} \qquad (2)$$

Where W: the amount of the electrode dissolved (g), I: the current intensity (A), t: the time (seconds), M: the relative molar mass of the electrode, z: the number of electrons in the redox reaction, and F: Faraday’s constant (96500 coulombs). At equilibrium, a relationship exists between the concentration of the NO_3^- species in solution and the concentration of NO_3^- species in the adsorbent (i.e. the amount of species adsorbed per unit mass of adsorbent). The amount of NO^{3-} at equilibrium on coagulant species q_e (mg/g) was calculated from the following equation (Kumar et al., 2010, Malakootian et al., 2011):

$$q_e = V \times (\frac{C_0 - C_e}{W}) \qquad (3)$$

6. Results and Discussion

6.1 Effect of Current Density and Time

The variation of percentage NO_3^- removal on the electrolysis time at different current densities has been shown in figure (2). It can be shown from figure (2) that the percentage NO_3^- removal increases with an increase in the electrolysis time for iron anodes. At the beginning of electrocoagulation process the percentage NO_3^- removal is sharp and it is increased regularly beyond 60 minutes, then it descent slowly to approach equilibrium. The plot shows that more than 88% of NO_3^- has been removed within 70 minutes by applying 10 mA/cm^2 current density. The NO_3^- residual concentration was about 18 mg/l (the drinking water standard limited $NO_3^- \leq$ 50 mg/l, (Emamjomeh and Sivakumar, 2009). Also, it can be shown that the increase of current density will increase NO_3^- removal. This can be explained that the extent of anodic dissolution of Fe metal increases at high current density resulting in great amount of flocs precipitate according to Faraday's law. However, the initial NO_3^- and pH are 150 mg/l, 8 respectively.

6.2 Effect of NaCl addition

NaCl was used as the supportive electrolyte with 200 mg/l concentration, because it increase conductivity of the solution and thus it reduces the energy consumption (YingHao Liu et al., 2011). With addition of NaCl to the NO_3^- solution, chlorine formed at the anode and it is then converted to hypochlorous acid and hypochlorite (Miao Li et al. 2010, Rezaee A. et al. 2011, YingHao Liu et al. 2011) and the following reactions take place:

$$2Cl^- \rightarrow Cl_2 + 2e^-$$

$$Cl_{2(g)} + H_2O \rightarrow HOCl + H^+ + Cl^-$$

$$HOCl \rightarrow ClO^- + H^+$$

The reduction of NO_3^- to N_2 gas is possible during the EC process and nitrate removal can occur with precipitation of metal hydroxide (Rezaee A. et al., 2011, Emamjomeh et al., 2009). The maximum removal efficiency of NO_3^- was achieved at high pH values because of the transformation of NO_3^- to other species, such as:

$$NO_3^- + 6H_2O + 8e^- \rightarrow NH_3 + 9OH^-$$

The hypochlorite acid formed would be oxidized by the product ammonia, and the nitrate was assumed to be reduced into nitrogen gas:

$$2NH_4^- + 3HOCl \rightarrow N_2 + 3H_2O + 5H^+ + 3Cl^-$$

As ammonia formation was decreased by the addition of NaCl, the total nitrogen sharply was decreased comparing to that without the addition of NaCl.

6.3 Kinetic Models

The kinetic studies describe the rate of adsorption of NO_3^- and this rate controls the equilibrium time. These kinetic models are useful for the design and optimization of effluent treatment models (Theivarasu and Mylsamy, 2010). To examine the controlling rates of adsorption process Langergren pseudo-first order kinetic model, Ho pseudo-second order kinetic and Elovich model are used to test the experimental data.

6.3.1 Pseudo-First Order Kinetic Model

The adsorption rate of adsorbate to given adsorbent is proportional to the amount of material adsorbed from solution. Pseudo-first order Langergren's model (Malakootain et al., 2011, Nemr, 2009, Theivarasu and Mylsamy, 2010) can be expressed as:

$$\frac{dq}{dt} = k_1(q_e - q_t) \qquad (4)$$

Where; k_1 is the pseudo-first order constant (min^{-1}).
q_t is the amount of adsorbate per unit mass of adsorbent at contact time t (mg/g).
q_e is the amount of adsorbate per unit mass of adsorbent at equilibrium (mg/g).
By integration at definite condition (t=0, q=0 and t=t, $q=q_t$), eq. (4) becomes:

$$\ln(q_e - q_t) = \ln q_e - k_1 t \qquad (5)$$

The adsorption rate constant k_1 can be experimentally determined by the slope of linear plots $\ln(q_e-q_t)$ vs. t. The data of NO_3^- adsorption onto ferric coagulant at various current densities applied to pseudo first-order model is shown in figure (3). The applicability of Langergren model supposes the formation of a monomolecular layer of NO_3^- species onto the surface of ferric coagulant. To investigate the influence of current density on pseudo-first order rate constant, table (1) shows the rate constant increases with the increase in current density. The first order model does not fit well with higher range of current density and it is applicable over the initial range.

6.3.2 Pseudo-Second Order Kinetic Model

The rate of adsorption for modified pseudo-second order Ho's model (Malakootain et al., 2011, Nemr, 2009, Theivarasu and Mylsamy, 2010) can be expressed as:

$$\frac{dq}{dt} = k_2(q_e - q_t)^2 \qquad (6)$$

Where; k_2 is the rate constant of the pseudo-second order reaction (g $mg^{-1}min^{-1}$).
Integration equation (6) for the boundary condition (t=0, q=0 and t=t, $q=q_t$), gives:

$$\frac{1}{(q_e - q_t)} = \frac{1}{q_e} + k_2 t \qquad (7)$$

Equation (7) has a linear form of:

$$\frac{t}{q_t} = \frac{1}{k_2 q_e^2} + \frac{1}{q_e} t \qquad (8)$$

k_2 and q_e can be obtained from the intercept and slope of plotting t/qt vs. t. The data of NO_3^- adsorption onto ferric coagulant at various current densities applied to pseudo-second order model is shown in Figure (4). The straight lines show high correlation coefficients exceeding 94% when pseudo-second order equation was applied and it is possible to ascertain that the rate determining process is a chemical reaction.

Table (1) shows the increase of pseudo-second rate constant with the increase in current density and higher values of correlation coefficient confirm that the process follows the pseudo-second order model . However the experiments show clearly that, the adsorbed NO_3^- at a fixed time increases with the increasing of current density, wherein such manner it has been observed that the produced ferric coagulant also increased dramatically with the increase of current density.

6.3.3 Elovich Kinetic Model

In reactions involving chemisorption of adsorbate on a solid surface without desorption of products, adsorption rate decreases with time due to an increased surface coverage. One of the most useful models for describing such activated chemisorption is the Elovich kinetic model (Ho and McKay, 1998, Hamdaoui and Chiha, 2007, G¨unay et al., 2007, Zohre Shahryari et al., 2010), the Elovich equation can be written as:

$$\frac{dq_t}{dt} = \alpha \exp(-\beta q_t) \qquad (9)$$

Where q_t is the sorption capacity at time t (mg/g), α is the initial sorption rate (mg g^{-1} min^{-1}) and β is the desorption constant (g mg^{-1}) during any one experiment (the extent of surface coverage and activation energy for chemisorption). To simplify the Elovich equation, an assumption of αβt >>1 and by applying the boundary conditions (t=0, q=0 and t=t, $q=q_t$) (Ho and McKay, 1998), gives:

$$q_t = \frac{1}{\beta}\ln(\alpha\beta) + \frac{1}{\beta}\ln t \qquad (10)$$

Our proposal for modified Elovich kinetic equation has the form:

$$-(q_e - q_t) = (\frac{1}{\beta}\ln(\alpha\beta) - q_e) + \frac{1}{\beta}\ln t \qquad (11)$$

Equation (11) has a linear form. A plot of $-(q_e-q_t)$ versus ln t gives a straight line with a slope of 1/ β and an intercept of (1/ β ln(α β)-q_e).

The data of NO^{3-} adsorption onto ferric coagulant at various current densities applied to Elovich kinetic model is shown in figure (5). The plot expresses the relation between the difference of adsorbed and equilibrium amounts of $NO3^-$ per the specific amounts of ferric coagulant against logarithmic time. The plot shows a linear relationship with good correlation coefficients except a current density of 2mA/cm^2. Table (1) exhibits the kinetic constants obtained from modified Elovich model. It will be seen from the result that the values of α and β vary as a function of current density. Thus an increasing current density decreases values of α (the initial adsorption rate), since the rate of coagulant generation increases rapidly and directly proportional to current density according to Faraday's law. The decreased value of α with the increases in current density extremely agreed with NO_3^- removal data (Fig.-2). While desorption constant β during any experiment, has been increased as the current density increased, which explains a higher agglomeration rate for NO_3^- ferric coagulant complex. The Elovich kinetic model has proved suitable for highly heterogeneous systems (Zohre Shahryari et al., 2010), of which adsorption of NO_3^- onto ferric coagulant is certainly such a case.

6.4 Adsorption Isotherms

It is assumed that the NO_3^- pollutant can act as a ligand to bind a hydrous iron in situ formed gelatinous precipitate. it is further attempted to extend the adsorption isotherm models for NO_3^- removal from aqueous solution. Analysis of the electrocoagulation experimental data resulted from the treated NO_3^- synthetic water based on Langmuir, Freundlich and Temkin isotherms can be predicted depending upon the varied anode current density and the mechanism of electrocoagulation. If W_{ad} is the mass of adsorbent produced, that can be taken constant for a given current density, hence the total mass of ferric coagulant produced within the electrolysis time (70 minutes) can be also estimated depending on current intensity with the application of Faraday’s law (equation 2) and the mass balance equation (3), and the molar mass difference between the dissolved Fe^o and the produced ferric coagulant. The NO_3^- amount that adsorbed on ferric coagulant can be expressed by q_e which represents the equilibrium milligrams of adsorbate (NO_3^-) per gram of adsorbent. Table (2) explains the amount of NO_3^- adsorbed on ferric coagulant.

6.4.1 Langmuir Adsorption Isotherm

The Langmuir isotherm assumes monolayer deposition of adsorbate on homogenous adsorbent surface. It is well known that the Langmuir equation is intended for a homogeneous surface. The mathematical expression of Langmuir isotherm (Chithra et al., 2008, Kumar et al., 2010, Malakootain et al., 2011, Zohre Shahryari et al., 2010, Theivarasu and Mylsamy, 2010) is given as:

$$q_e = (\frac{q_{Max} K_L C_e}{1 + K_L C_e}) \qquad (12)$$

Where q_e is the solid phase adsorbate concentration in equilibrium (mg/g), q_{max} is the maximum adsorption capacity corresponding to complete monolayer coverage on the surface (mg/g), C_e is the concentration of adsorbate at equilibrium (mg/l), and K_L is the Langmuir constant (l/g). Equation (10) can be rearranged to a linear form:

$$\frac{C_e}{q_e} = \frac{1}{q_{Max} K_L} + \frac{C_e}{q_{Max}} \qquad (13)$$

Accordingly, a plot of C_e/q_e vs. C_e produce a straight line with a slope of $1/q_{max}$ and intercept of $1/(K_L\ q_{max})$. The plot of Langmuir adsorption isotherm for NO_3^-/ferric coagulant system is shown in figure (6). The maximum adsorption capacity q_{max} value was found to be comparable with other adsorbents, and the results are given in table (3). However the calculated value of linear correlation coefficient indicates a less fit applicability of Langmuir isotherm compared with other isotherms.

6.4.2 Freundlich Adsorption Isotherm

It is empirical model relating the adsorption intensity of the sorbent towards adsorbent. The isotherm describes the multilayer adsorption with a heterogeneous energetic distribution of active sites, accomplished by interaction between adsorbed molecules. The mathematical expression of Freundlich isotherm (Chithra et al., 2008, Kumar et al., 2010, Malakootain et al., 2011, Zohre Shahryari et al., 2010, Theivarasu and Mylsamy, 2010) is represented by:

$$q_e = K_F\ C_e^{\frac{1}{n}} \qquad (14)$$

K_F is Freundlich constant that indicate the adsorption capacity of the adsorbent (l/gm) and n is an empirical constant related to the magnitude of the adsorption driving force. The Freundlich isotherm can be rearranged to give a linear form:

$$Ln(q_e) = Ln(K_F) + \frac{1}{n} Ln(C_e) \qquad (15)$$

Accordingly, a plot of $\ln(q_e)$ vs. $Ln(C_e)$ produces a straight line with a slope of 1/n and intercept of $\ln(K_F)$. Freundlich plot for the adsorption of logarithmic NO_3^-/ferric coagulant versus the logarithmic equilibrium concentration is shown in figure (7) and the results of such plot are given in table-3. It shows that the value of adsorption intensity is $1/n < 1$ exhibit that the applicability of Freundlich adsorption is the best fit compared to other adsorption isotherms. The highest calculated value of linear correlation coefficient confirms this result.

6.4.3 Temkin Adsorption Isotherm

The Temkin isotherm describes the behavior of adsorption system on heterogeneous surface (Chithra et al., 2008, Kumar et al., 2010, Malakootain et al., 2011, Zohre Shahryari et al., 2010, Theivarasu and Mylsamy, 2010) and represented as follow:

$$q_e = \frac{RT}{b_0} Ln(K_T C_e) \qquad (16)$$

Equation (16) can be expressed in a linear form as:

$$q_e = BLn(K_T) + BLn(C_e) \qquad (17)$$

Where $B = RT/b_0$, and B is a constant related to adsorption heat, and K_T is the equilibrium binding Temkin constant (l/gm) corresponding to maximum binding energy. A plot of q_e vs. Ln(Ce) enables to determine the constants B and K_T. Temkin plot for the adsorption of NO_3^-/ ferric coagulant versus logarithmic time is shown in figure (8) and the results of a such plot are given in table (3). However, the isotherm accord a less fit to describe equilibrium data with low estimated linear correlation coefficient, compared to Freundlich isotherm. Figure (7) and table (3) show that the NO_3^- experimental equilibrium measurement gives acceptable analogous along with Freundlich adsorption isotherm having a linear correlation coefficient (R_2) of 0.9671, compared with lesser value for both Langmuir and Temkin adsorption isotherms.

However, the variation between the adsorption isotherms of NO_3^-/ferric coagulant system analysis was illustrated by the two parameters for each isotherm that supported their assumption principles. Consequently, this investigation satisfies that the Freundlich isotherm, even though it is an empirical model, can relate the adsorption intensity of NO_3^- towards ferric coagulant from an aqueous solution.

7. Conclusion

Experiments were carried out to treat synthetic sodium nitrate water with sodium chloride salt as a supportive electrolyte by EC technique to find the feasibility of NO_3^- adsorption on ferric coagulant with four MP-P electrode connections. EC technique produces an acceptable result using a covering range of current density and electrolysis time operating conditions to remove NO_3^- pollutant. For equipment design purposes and process optimization of NO_3^- effluent treatment, the data of electrocoagulation is subjected to the kinetic rate model equations to examine the controlling rate of adsorption process. Moreover, the equilibrium data is subjected to the adsorption isotherms to analyze the mechanism of adsorption. The following conclusions can be made from the present investigation:

1. The process of electrocoagulation of NO_3^- removal by ferric coagulant is influenced by the applied current density and the electrocoagulation time. The percentage of NO_3^- removal increases with an increase in the applied current density and electrolysis time for iron anode.
2. The rate controlling kinetic of NO_3^-/ferric coagulant system with the generation of Fe(III) can be described by pseudo second order model which offered a better fit of NO_3^- removal experimental data in comparison with Elovich and the pseudo first order models.
3. It has been ascertained that Freundlich adsorption isotherm match satisfactorily with the equilibrium experimental results to describe the electrocoagulation mechanism of NO_3^- removal by ferric coagulant in comparison with Langmuir and Temkin isotherms.

Acknowledgements

The authors would like to thank the Electrochemical Engineering Department of Babylon University for supporting and approving this research. They also appreciate Mr. Muhanad for his help.

References

APHA (American Public Health Association), (2000), Standard Methods for the Examination of Water and Wastewater. 20th ed. Washing, DC., USA.

Balasubramanian, N.; Kojima, T.; Srinivasakannan, C., (2009), Arsenic removal through electrocoagulation: Kinetic and statistical modeling. Chem. Eng. J., 155, 76-82.

Canter L.W., Nitrates in Groundwater. Lewis Publishers, New York 1997.

Can, O.T., Kobya, M., Demirbas, E. and Bayramoglu, M., (2006), Treatment of the textile wastewater by combined electrocoagulation. Chemosphere, 62: 181 – 187.

Canizares P., Martínez F., Jiménez C., Lobato J., Rodrigo M. A., Env. Sci. Tech. 40, (2006) 6418.

Chithra, K., Balasubramanian, N., (2010), Modeling Electrocoagulation Through Adsorption Kinetics, J. of Modeling and Simulation of Systems (Vol.1-2010/Iss.2) pp. 124-130.

El-Shazly A.H., Al-Zahrani A.A., Al-Shahrani S.S., 2011, Improvement of NO_3^- Removal from Wastewater by Using Batch Electrocoagulation Unit with Vertical Monopolar Al Electrodes. Int. J. Electrochem. Sci. (6) 4141 – 4149.

Emamjomeh, M.; Sivakumar, M., 2009, Denitrification using a monopolarelectrocoagulation/flotation (ECF) process, Journal of Environmental Management Vol. 91 No. 2 pp. 516-522.

G¨unay A, Arsalnkaya E, Tosun I (2007), Lead Removal from Aqueous Solution by Natural and pretreated Clinoptilolite: Adsorption Equilibrium and Kinetic, J. Hazard. Mater. 146:362-371.

Goran Robic and Everson Alves Miranda, (2010), Modeling of Protein and Phenolic Compound Removal from Aqueous Solutions by Electrocoagulation, Biotechnol. Prog., Vol. 26, No. 1

Hamdaoui O, Chiha M (2007), Removal of Methylene Blue from Aqueous Solutions by Wheat Bran , Act Chim. Slov. 54, 407-418.

Ho Y. S. and McKay G., 1998, Comparison of chemisorption kinetic models applied to pollutant removal on various sorbents, Trans I Chem.Eng., Vol 76, Part B.

Horold S., Tacke T., Vorlop K., Environ. Technol. 14, (1993) 931.

Kay W. Canton, Fluid waste disposal (2010), Published by Nova Science Publishers, Inc.

Kumar, P.S., Ramakrishnan, K., Kirupha, S.D., (2010), Thermodynamic and Kinetic Studies of Cadmium Adsorption from Aqueous Solution onto Rice Husk Braz. J. chem. Eng. Vol. 27 no.2.

Koparal, A.,S., Ogutveren, U.B., (2002), Removal of nitrate from water by electroreduction and electrocoagulation, J.Hazard. Mater. 4;89, 83–94.

Liang S., Mann M.A., Guter G.A., Kim P.H., Hardan D.L., J. Am. Water Works Assoc. 91 (2), (1999) 79.

Lin, S.; Wu, C., (1996), Electrochemical removal of nitrite and ammonia for aquaculture. Water Res., 30, 715 – 721

Luk, G.; Au-Yeung,W., (2002), Experimental investigation on the chemical reduction of nitrate from groundwater. Adv. Environ. Res., 6, 441 – 453.

Miao Lia, Chuanping Fenga, Zhenya Zhangb, Rongzhi Chenb, Qiang Xueb, Chengjie Gaoc, Norio Sugiurab, 2010, Optimization of process parameters for electrochemical nitrate removal using Box–Behnken design, Electrochimica Acta, 56 (265–270).

Mollah M.Y.A., Morkovsky, P., Gomes, J. A., Kesmez, M., Parga, J., and Cocke, D. L., 2004. Fundamentals, Present and Future Perspectives of Electrocoagulation. J. of Hazard. Mater., B114: 199 – 210.

Malakootian M., Yousefim N., Fatehizadeh A., 2011. Survey efficiency of electrocoagulation on nitrate removal from aqueous solution, Int. J. Environ. Sci. Tech., 8 (1), 107-114.

Mehmet Uğurlu, (2004).The Removal of Some Inorganic Compounds from Paper Mill Efflunts by The Electrocoagulation Method, G.U. Journal of Science 17(3):85-99.

Mohammed ALHassan and M. A. Olutoye, (2006), Mathematical Modeling of a Simulated Fixed Bed for Desalting Operation Leonardo Journal of Sciences ISSN 1583-0233 Issue8, January-June2006p.21-32.

Malakootain, M., Moosazadeh, M., Yousefi, N., Fatehizadeh, A., (2011), Fluoride Removal from Aqueous Solution by Pumice, African J. of Environ. Science and Technology Vol. 5(4), pp.299-306.

Nemr A E, (2009), Potential of Pomegranate Husk Carbon for Cr(VI) Removal from Wastewater: Kinetic and Isotherm Studies, J. Hazard. Mater., 161: 132-141.

Nese Öztűrk, T. Enil Köse, 2008, a kinetic study of nitrate adsorption onto sepiolite and powdered activated carbon, Desalination 223, 174-179.

Parga, J. R., Vazquez, V., and Moreno, H., (2009), Thermodynamic Studies of the Arsenic Adsorption on Iron Species Generated by Electrocoagulation Journal of Metallurgy Volume 2009, Article ID 86971, 9, pages doi:10.1155/2009/286971.

Parga, J. R. , Cocke, D. L. Valverde, V., (2005), Characterization of electrocoagulation for removal of chromium and arsenic, Chemical Engineering and Technology, vol. 28, no. 5, pp. 605–612.

Prasad P.K., Priya M.N.and Palanivelu K., 2005, Nitrate Removal from Groundwater Using Electrolytic Reduction Method. Indian Journal of Chem. Technology, Vol.12, pp. 164-169.

Rezaee A., Hossini H., Mosoumbeigi H., Soltani R., (2011), Simulataneous Removal of Hexavalent Chromium and Nitrate from Wastewater Using Electrocoagulation method, I. J. of Environmental Science and Development, Vol. 2, N o.4.

Shahryari Z., Goharrizi A. S., Azadi M., (2010), Experimental Study on Methylene Blue Adsorption from Aqueous solution onto carbon Nano Tubes, Inter. J. of Water and Environ. Eng. Vol.2(2), pp16-28.

Sudipta Chatterjee, Dae S. Lee, Min W. Lee and Seung H. Woo, 2009, nitrate removal from aqueous solutions by cross-linked chitosan beads conditioned with s. bisulfate, J. of Hazardous Mat. 166, 508-513.

Theivarasu C., Mylsamy S., 2010, equilibrium and kinetic adsorption studies of Rhodamine-B from aqueous solutions using cocoa shell as new adsorbent, Int. J. of Engg. Science and Tech., Vol.2(11), 6284-6292.

Wei Wan, The Arsenic Removal from Drinking Water by Electrocoagulation, May 2010, M Sc Thesis School of Engineering, Saint Louis, Missouri, Washington University.

YingHao Liu, Sanjay Kumar, JungHoon Kwag, JaeHwan Kim, JeongDae Kim, Changsix Ra, 2011, Recycle of Electrolytically Dissolved Struvite as Alternative to Enhance Phosphate and Nitrogen Recovery from Swine Wastewater, J. of Hazardous Materials, 195, 175-181.

Zohre Shahryari, Ataallah Soltani Goharrizi, Mehdi Azadi, (2010), Experimental Study on Methylene Blue Adsorption from Aqueous solution onto carbon Nano Tubes, Inter. J. of Water and Environ. Eng. Vol 2 (2), pp016-028.

Author(s)

Ghanim, A., N., Asst. Professor, Department of Electrochemical Engineering, Engineering College, Babylon University, Hilla, Iraq. Email: ala_gh2003@yahoo.com

Ajjam, S., K., Asst. Professor, Department of Electrochemical Engineering, Engineering College, Babylon University, Hilla, Iraq. Email: satajam58@yahoo.com

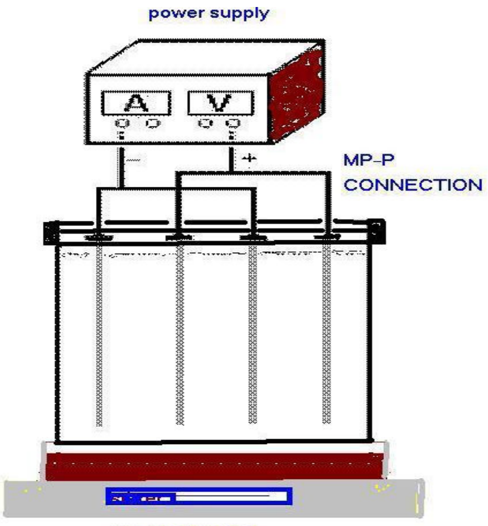

Fig.1 Schematic of MP–P Nitrate Treatment Set-Up

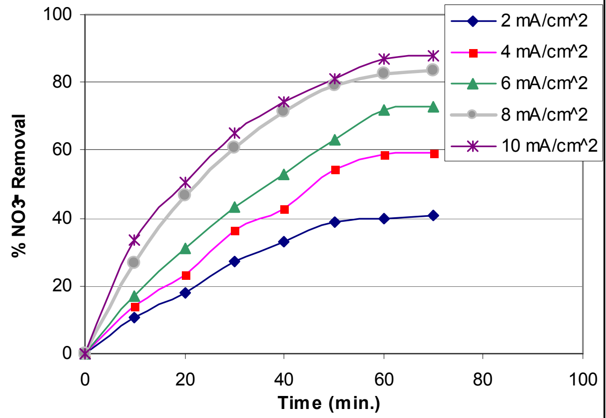

Fig.2 Variation of % NO3− Removal with Current Density and Electrocoagulation Time

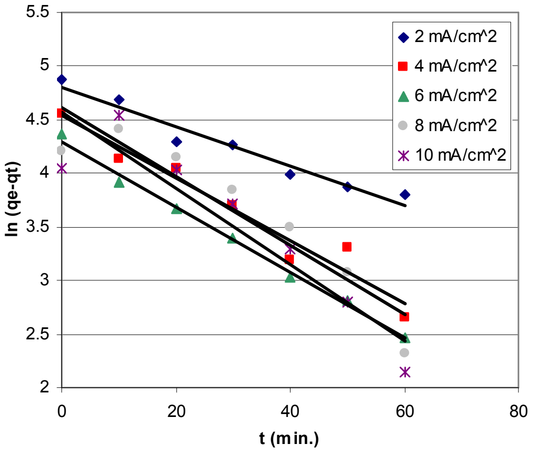

Fig.3 Modeling NO3− Electrocoagulaion (Pseudo First Order)

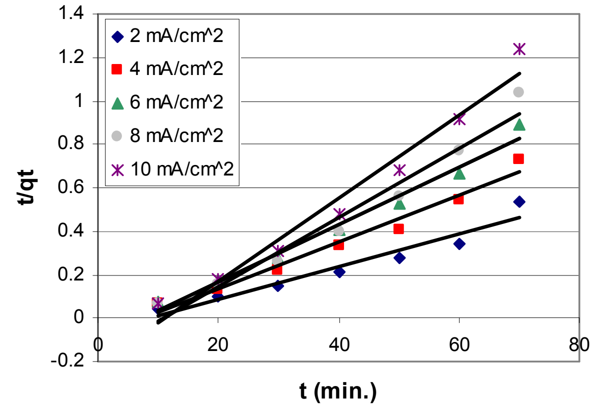

Fig.4 Modeling NO3− Electrocoagulation (Pseudo-Second Order)

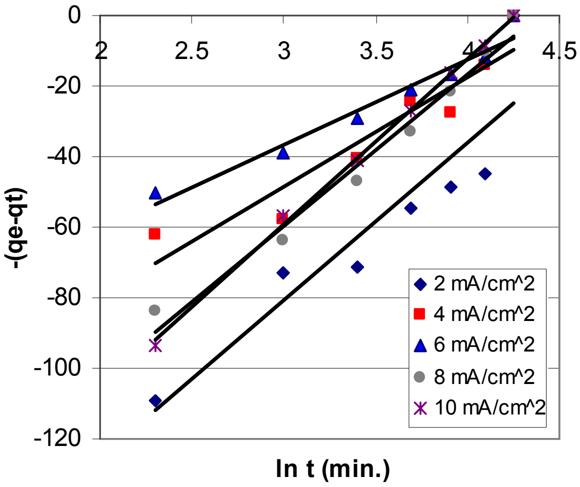

Fig. 5 Modeling NO3− Electrocoagulation (Elovich Model)

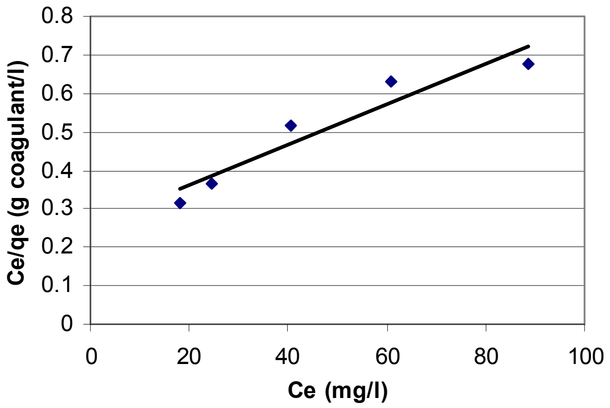

Fig.6 Langmuir NO3− Adsorption Isotherm

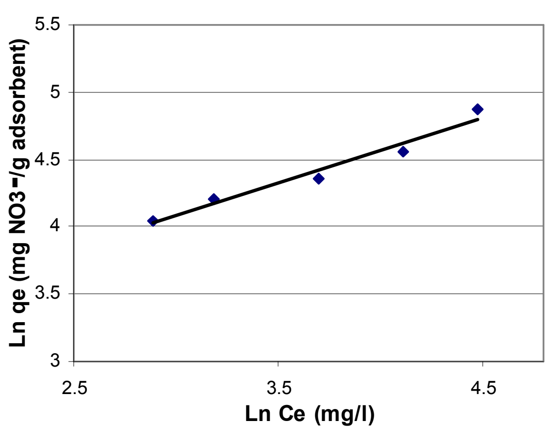

Fig.7 Freundlich NO3– Adsorption Isotherm

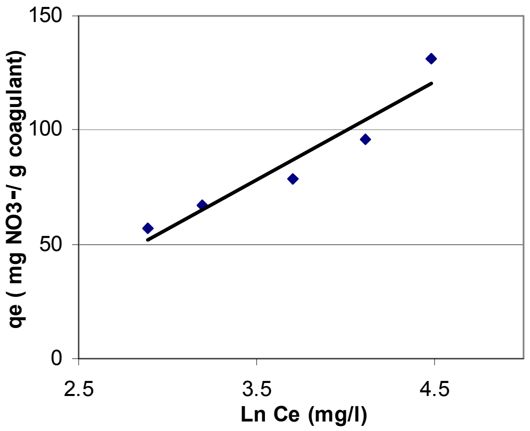

Fig.8 Temkin NO3– Adsorption Isotherm

***Table (1)** Kinetic models values for adsorption of NO_3^- onto ferric coagulant.*

Current Density mA/cm^2	Pseudo-First Order			Pseudo-Second Order			Elovich		
	K_1	q_e	R^2	K_2	q_e(calc.)	R^2	α	β	R^2
2	0.0183	131.5	0.9526	0.00088	135.1	0.9498	7.02	0.0224	0.8443
4	0.0293	95.7	0.9500	0.00140	92.6	0.9746	6.97	0.0320	0.8950
6	0.0306	78.4	0.9952	0.00181	75.7	0.9806	6.71	0.0409	0.9599
8	0.0321	67.4	0.8733	0.00210	62.9	0.9645	2.58	0.0432	0.9775
10	0.0355	56.7	0.8617	0.00241	52.1	0.9696	2.23	0.0450	0.9983

***Table (2)** Nitrate milligrams adsorbed on ferric coagulant(q_e)*

C.D. mA/cm^2	Equilibrium NO_3^- C_e, (mg/l)	W_{ad} (g)	q_e (mg/g)
2	88.70	0.4657	131.5
4	60.90	0.9314	95.7
6	40.50	1.3970	78.4
8	24.50	1.8628	67.4
10	18.00	2.3285	56.7

***Table (3)** Parameters of Langmuir, Freundlichr and Temkin isotherm constants and correlation coefficients.*

Isotherm	R^2	constant	Value
Langmuir	0.9106	K_L (l/g) q_{max}(mg/g)	20.20 192.3
Freundlich	0.9671	K_F (l/g) n	13.6 2.05
Temkin	0.9125	K_T (l/g) B	0.187 43.03

This academic article was published by The International Institute for Science, Technology and Education (IISTE). The IISTE is a pioneer in the Open Access Publishing service based in the U.S. and Europe. The aim of the institute is Accelerating Global Knowledge Sharing.

More information about the publisher can be found in the IISTE's homepage:
http://www.iiste.org

CALL FOR PAPERS

The IISTE is currently hosting more than 30 peer-reviewed academic journals and collaborating with academic institutions around the world. There's no deadline for submission. **Prospective authors of IISTE journals can find the submission instruction on the following page:** http://www.iiste.org/Journals/

The IISTE editorial team promises to the review and publish all the qualified submissions in a **fast** manner. All the journals articles are available online to the readers all over the world without financial, legal, or technical barriers other than those inseparable from gaining access to the internet itself. Printed version of the journals is also available upon request of readers and authors.

IISTE Knowledge Sharing Partners

EBSCO, Index Copernicus, Ulrich's Periodicals Directory, JournalTOCS, PKP Open Archives Harvester, Bielefeld Academic Search Engine, Elektronische Zeitschriftenbibliothek EZB, Open J-Gate, OCLC WorldCat, Universe Digtial Library , NewJour, Google Scholar